GFD 2006 Lecture 1: Introduction to Ice

Grae Worster; notes by Rachel Zammett and Devin Conroy

March 15, 2007

1   Introduction

Our aim in this course is to understand some of the processes associated with ice in the natural environment. Figure 1 shows the location of some of Earth's ice during the northern winter. These ice deposits may be categorized as sea ice, ice sheets and shelves, and permafrost.
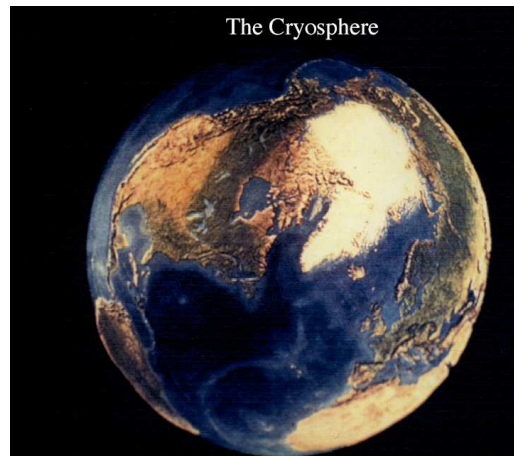

Figure 1: Satellite image showing the ice cover in the northern hemisphere during northern winter, showing sea ice lying in the Arctic basin, the permanent ice sheet over Greenland and permafrost in the exposed land surface.

2   Ice sheets

Firstly, figure 1 shows the ice sheet that covers approximately 80% of Greenland. This is about 10^5 years old and reaches depths of 2–3 kilometers. On large scales, ice can be treated as a highly viscous, non-Newtonian fluid that can flow because it is a polycrystalline solid and contains a percentage of unfrozen water (figure 2). Looking on a scale of about $100\mu m$,
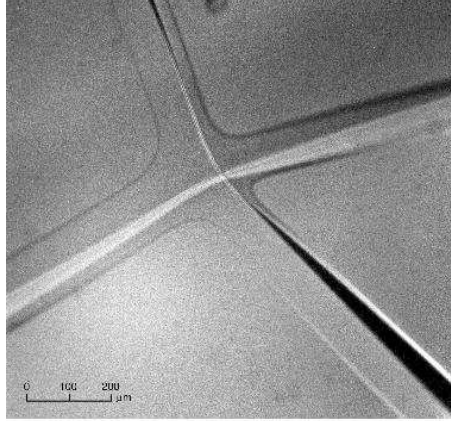
Figure 2: Image of the intersection of four ice grains. Between these grains lie the veins containing liquid water and dissolved impurities. The scale bar on this picture is 100 μm.

we can see the ice grain junctions and the veins which lie between them. The liquid water contained in the veins between the ice crystals lubricates the flow, allowing the ice to flow more easily. This water can also transport dissolved impurities, which will therefore move relative to the ice crystals; this is important when analyzing ice cores, for example.

Figure 2 also shows that there is a curvature to the solid–liquid interface which is associated with the surface energy of the phase boundary. We will see later that this surface energy sets the scales for morphological instabilities of the solid–liquid interface, such as those seen in snowflakes (figure 4).

The grounded ice cap flows slowly towards the coast, sometimes flowing into floating ice shelves, which ultimately break up to form icebergs. Projects such as the Greenland Ice Core Project (GRIP) have obtained deep ice cores from near Greenland's summit. Analyzing the properties of the ice cores, such as oxygen isotope ratios, allow inferences about the ancient climate to be drawn.

In figure 3 we see the flow from the grounded ice sheet to a floating ice shelf (Larsen B) in Antarctica. At the edge of the ice shelf we see the calving of icebergs; this is responsible for approximately 80% of the mass lost from Antarctica. The icebergs are composed predominantly of freshwater ice, as the ice which comprises the ice sheets first fell as snow. Owing to the density difference between water and ice, approximately 90% of the volume of an iceberg is below the surface of the ocean.

When these icebergs come into contact with the warm, salty ocean they ablate, providing a freshwater flux to the ocean. This is important as the production of deep ocean waters is sensitive to changes in the freshwater budget.

3   Sea ice

Secondly, there is the sea ice which fills the Arctic basin and is formed by direct freezing of the ocean. It is typically 1–3 m thick and less than 10 years old; in its first year, sea

Figure 3: (left) Satellite image of the Larsen B ice shelf on the coast of Antarctica. Near the edge of the ice shelf, it is possible to see the icebergs formed by calving. (right) An example of an iceberg formed by calving at the edge of an ice sheet or ice shelf. Here the vertical face is 30 m above the surface of the ocean, meaning that approximately 300 m of ice lie below the surface.

ice typically grows to a depth of 1 m. This relative youth (in comparison to ice sheets or glaciers, for example) is caused by the movement of sea ice by polar winds and ocean currents to warmer waters, where it melts.

Many of the structures and processes observed in sea ice develop because the thermal diffusivity of heat is much larger than the diffusivity of salt. In this course we shall see that sea ice can be considered as an inhomogeneous porous medium. While sheet ice only contains water in the veins between ice crystals, sea ice has a much higher porosity (approximately 10 % in old ice and up to 40 % in new ice). The porous nature of sea ice means that it can also be modified by internal convection.

We shall consider sea ice to be a mushy layer, which is a two-phase reactive porous medium. We see in figure 4 that it is not macroscopically solid; instead, it is composed of ice platelets with salty brine between them. The platelets which form are composed of pure ice crystals, as the crystals reject the salt contained in the ocean water. Some of this rejected salt convects into the ocean below the sea ice, and the rest remains between the crystals.

This convection is also seen in the laboratory. Figure 5 shows shadowgraph pictures of sea ice growing in a laboratory. In figure 5 (left) when the sea ice is only 3 cm thick, it is possible to see some convection occurring in the salt water below it, but it is small scale and has no obvious structure. However, when the ice has grown to a thickness of about 13 cm (figure 5), it is possible to see strong convective plumes in the water below. These have a high salt content and therefore deliver a large flux of salt to the water below. We shall see that there is a critical ice thickness at which such plumes occur; this criterion for the onset of convection is determined by a form of Rayleigh number.
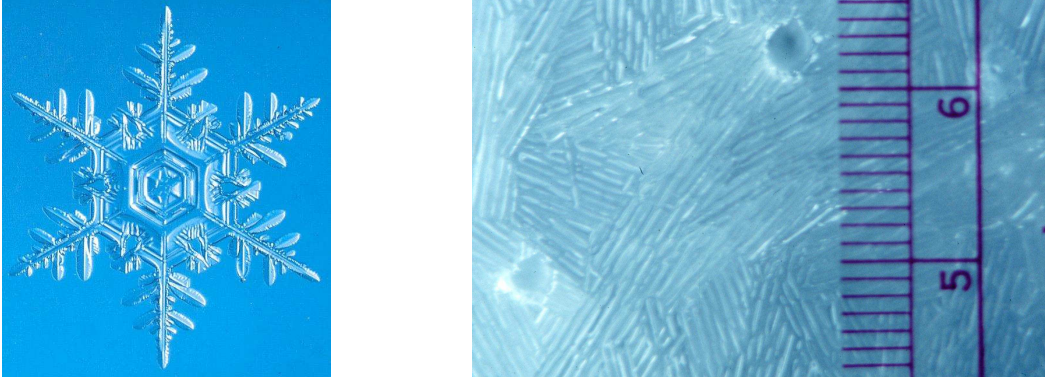
Figure 4: (left) Picture of a snowflake. Here the smallest scale at which instabilities occur is comparable to the radius of the tip of one of the needles. (right) Horizontal cross section of sea ice, showing both ice platelets and brine channels. The ice platelets are typically less than 1 mm wide and form a porous matrix, which allows convection and the erosion of such channels by the rejection of salt. These channels have a diameter of a few millimetres.
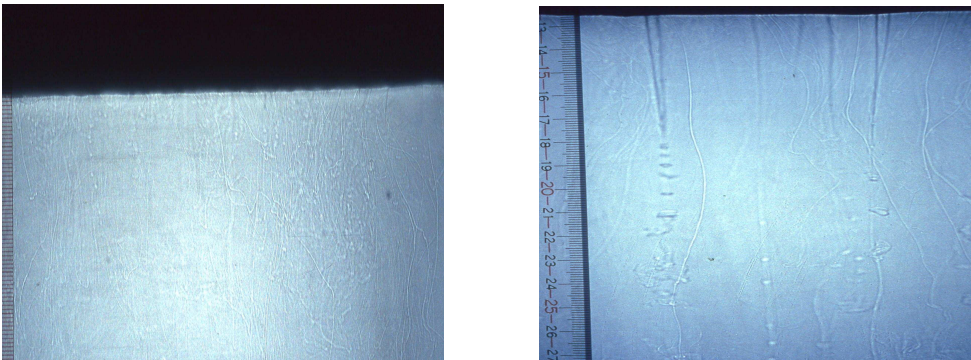

Figure 5: (left) Image of sea ice growing in the laboratory. At this time, the layer of ice (the dark upper region) is 3 cm thick, and it is possible to see some convection occurring below it. (right) Image of sea ice growing in the laboratory where the layer of ice is now 13 cm thick, and it is possible to see the salty convective plumes below it. It is also possible to see the 'pinching' instability at the base of these plumes. Note that the scales of the images are different.
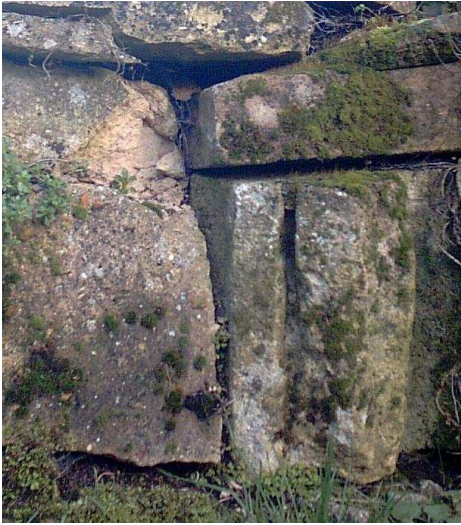
4

Figure 6: (left) An example of erosion caused to a rockery by winter frost. (right) Stone circles as an example of differential frost heave.
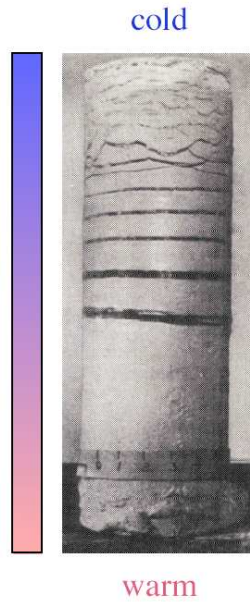

cold

warm

Figure 7: (left) Ice needles protruding from soil. (right) Photograph of a column of water-saturated soil cooled at the top (Taber, 1929). The black regions are ice lenses, which contain no soil; between these are regions of partially frozen soil. There may also be ice between the soil particles below the lowest lens.

4　Permafrost

The final type of ice we shall consider is permafrost, or permanently frozen ground (defined as remaining below 0°C for more than two years). It occurs both on land and beneath offshore Arctic continental shelves, and its thickness ranges from less than one meter to greater than 1 kilometer. Permafrost underlies about 15% of the exposed land surface in the Northern Hemisphere and causes deformation of the ground; we shall be looking at this and the associated flows.

Figure 6 shows the effects of ice damage to rocks and buildings if they are eroded by winter frost. The ground may also 'heave', i. e. rise upwards due to water being pulled up from the unfrozen ground below. Differential frost heave may form patterned ground, such as hummocks and the stone circles seen in figure 6. Underlying this is the force of separation between ice and other materials: in this context, we will consider the other materials to be silicates. We will consider how ice pushes on another material forming, for example, the ice needles seen in figure 7.

There are still some puzzles remaining. Figure 7 shows a laboratory experiment by Taber where a column of water-saturated soil was frozen by cooling at its top. It might be expected that a freezing front which moves downwards is observed, but instead a sequence of layers of alternating pure ice and partially frozen soil forms.

5　Student Problem

If two identical ice cubes are placed in glasses of water and whisky, where the liquids are at the same temperature, it is observed that the ice cube in the whisky melts more quickly than that in the water. Why? (Hint: It is not because the melting point of ice is lower in whisky than in water.)

Answer

Initially when the ice cube is placed into a glass of whisky at room temperature the ice melts, forming a layer of cold freshwater adjacent to the phase boundary. Since water is denser than alcohol and the the melted water is colder than the whisky, a plume forms that convects the cool fresh water downwards and brings warmer fluid with a higher alcohol concentration upwards. This convective mixing of the liquid below the ice cube supplies a heat flux at the phase boundary; this flux is stronger than the diffusive heat flux in the absence of convection.

6　Stefan Condition

The distinguishing feature of solidification or melting is the evolution of a phase boundary which separates solid and liquid. The speed of this interface can be determined by energy conservation, as illustrated in figure 8, which relates the rate of energy absorption or release to the difference in heat fluxes across this boundary. This is formulated mathematically as follows by considering a control volume around the phase boundary

$$\mathbf{q_s} \cdot \mathbf{n} - \mathbf{q_l} \cdot \mathbf{n} - \rho V_n H_s + \rho V_n H_\ell = 0 \Rightarrow \rho L V_n = \mathbf{n} \cdot (\mathbf{q_l} - \mathbf{q_s}). \tag{1}$$
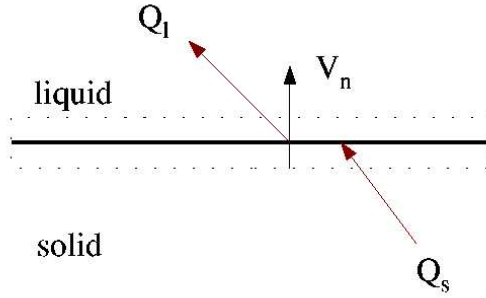
Figure 8: Illustration showing the control volume taken around the phase boundary and the energy fluxes into and out of it.

Here $\mathbf{q} = -k\nabla T$ is the heat flux from Fourier's law, k is thermal conductivity, $\mathbf{n}$ is the unit normal vector pointing from solid to liquid, ρ is the density (assumed to be the same in each phase), V_n the interface velocity, H is the enthalpy, $L = H_\ell - H_s$ is the latent heat and subscripts s and ℓ denote solid and liquid respectively. We assume that the phase boundary is in equilibrium, implying that the temperature is constant on either side of the interface. This equation is known as the Stefan condition, attributed to Stefan in 1891.

7 Problem 1

We consider a problem posed by Stefan in 1891, where solid ice is growing into relatively warm $(T_m > T_B)$ water from a cooled boundary at $z = 0$ (figure 9). We assume that the liquid portion is at the melting temperature T_m initially and therefore remains at this temperature. The governing equation is given by the thermal diffusion equation

$$\rho c_p \frac{\partial T}{\partial t} = \frac{\partial}{\partial z}\left(k\frac{\partial T}{\partial z}\right) \Rightarrow \frac{\partial T}{\partial t} = \kappa\frac{\partial^2 T}{\partial t^2}, \tag{2}$$

where the conductivity $k = \rho c_p \kappa$ is assumed to be constant and the thermal diffusivity is represented by κ. The boundary conditions for this equation are then

$$T(t, z = 0) = T_B, \qquad T(t, z = a(t)) = T_m, \tag{3}$$

where $z = a(t)$ denotes the interface position and the unknown interface velocity is determined by the Stefan condition

$$\rho L \frac{\mathrm{d}a}{\mathrm{d}t} = k\left.\frac{\partial T}{\partial z}\right|_{z=a(t)}. \tag{4}$$

7.1 Solution

This problem can be solved using a similarity solution, as there is no intrinsic length scale in the problem. We can determine the form of this similarity variable using a scaling analysis
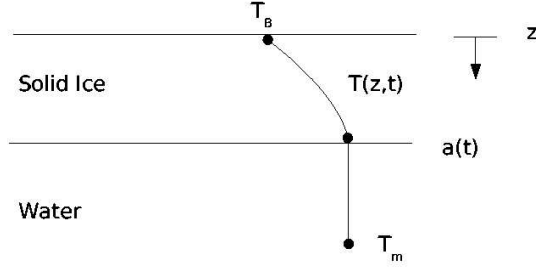
7

Figure 9: Growth of a planar solid into a liquid, maintained at the melting temperature T_m from a cooled boundary maintained at temperature T_B. The position of the interface as a function of time is given by $a(t)$.

and show that a fixed length scale cannot be formed. Let us define the appropriate scales, $\Delta T = T_m - T_B$, D and τ for the temperature, length of the domain and time respectively. From the diffusion equation (2) and the Stefan condition (8) we obtain the following

$$\frac{\Delta T}{\tau} \sim \kappa \frac{\Delta T}{D^2} \Rightarrow D \sim \sqrt{\kappa \tau}, \tag{5}$$

$$\rho L \frac{D}{\tau} \sim k \frac{\Delta T}{D} = \rho c_p \kappa \frac{\Delta}{D} T \Rightarrow D \sim \sqrt{\kappa \tau} S^{-1/2}, \tag{6}$$

where $S = L/(c_p \Delta T)$ is the Stefan number. Since the relationships between D and τ in (5) and (6) are the same, there is no intrinsic length scale, and a similarity solution is possible. In addition there therefore is no time scale so we choose $\tau = t$, the actual time, in which case $D \sim \sqrt{\kappa t}$.

We introduce the dimensionless variable f such that

$$T - T_B = \Delta T f \left(\frac{z}{D}, \frac{t}{\tau} \right) = \Delta T f \left(\frac{z}{\sqrt{\kappa t}}, 1 \right) = \Delta T f(\eta). \tag{7}$$

We choose $\eta = z/2\sqrt{\kappa t}$ for mathematical convenience, as the similarity variable may be multiplied by an arbitrary constant. In addition we know from scale analysis, using the diffusion equation, that length and therefore interface position can be assumed to have the form

$$a = 2\mu \sqrt{\kappa t}, \tag{8}$$

where the parameter μ must be determined as part of the solution. Rewriting the model in terms of the similarity variable, we arrive at the final set of non-dimensional equations

$$f'' = -2\eta f', \tag{9}$$
$$f(\eta = 0) = 0, \tag{10}$$
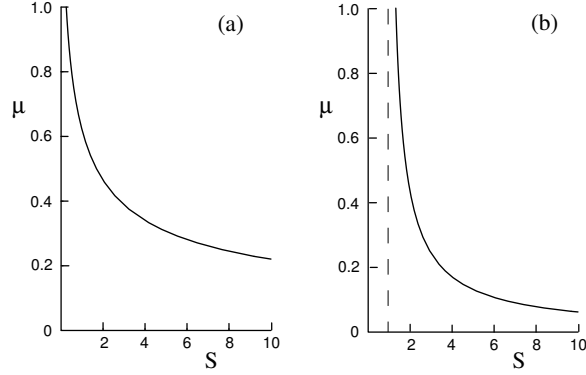$$f(\eta = \mu) = 1, \tag{11}$$
$$2 S \mu = f'(\eta = \mu). \tag{12}$$

8

Figure 10: (a) Solution to equation (17) for the eigenvalue μ as a function of the Stefan number, S. (b) Solution to equation (7) of Lecture 2.

The solution to equation (9) is determined using an integrating factor and determining

$$f' = c_1\, e^{-\eta^2} \Rightarrow f = c_1 \int_0^\eta e^{-y^2}\, dy + c_2 \Rightarrow f = \hat{c}_1 \mathrm{erf}(\eta) + c_2. \tag{13}$$

The error function, $\mathrm{erf}(\eta)$, is defined by

$$\mathrm{erf}(x) = \frac{2}{\sqrt{\pi}} \int_0^x e^{-u^2}\, du, \tag{14}$$

with the following properties

$$\mathrm{erf}(0) = 0, \tag{15}$$

$$\mathrm{erf}(\infty) = 1. \tag{16}$$

Boundary condition (10) implies that $c_2 = 0$ and boundary condition (11) gives $\hat{c}_1 = 1/\mathrm{erf}(\mu)$. Finally the Stefan condition (12) gives us an parameter equation to be solved for the parameter μ. From equation (12) we then have

$$\frac{1}{S} = \sqrt{\pi}\, \mu\, \mathrm{erf}(\mu)\, e^{\mu^2} = F(\mu). \tag{17}$$

In figure 10 we plot the parameter μ as a function of Stefan number. We see that the growth speed increases as the Stefan number decreases, which corresponds to increasing the driving temperature difference or decreasing the amount of energy required to melt a unit mass of solid. We should note that the interface position is given by $a \propto \sqrt{t}$ and the interface velocity by $\dot{a} \propto 1/\sqrt{t}$ so that the growth rate of a solid decreases with time.

7.2   Quasi Stationary Approximation

For large Stefan numbers we have relatively small sensible heat compared to latent heat and the growth rate will be slow compared to the thermal diffusion rate. In this case, the temperature field will evolve more rapidly than the boundary position and we have a quasi-steady state regime for the the diffusion equation. This implies a linear profile of the solid

9

temperature that is slowly decreasing in slope as the boundary moves. Integrating Laplace's equation twice and applying boundary conditions given in (3) we obtain the linear solution

$$T = T_B + (T_m - T_B)\frac{z}{a}. \tag{18}$$

Substituting this solution into the Stefan condition (12) we arrive at the following expression for the interface position a

$$a\frac{\mathrm{d}a}{\mathrm{d}t} = \frac{1}{S}, \qquad a(0) = 0 \qquad \Rightarrow a = \sqrt{\frac{2}{S}}\sqrt{\kappa t}. \tag{19}$$

8 Student Problem

Question

Solve the Stefan problem given in problem 1 for the case $\rho_s \neq \rho_\ell$.

Answer

When the density between the solid and liquid differ by an appreciable amount there will be a normal velocity to the phase change surface due to the expansion or contraction of the liquid as it solidifies. To formulate this effect mathematically we draw a control volume around the moving surface and conserve mass and energy as follow

$$\frac{\mathrm{d}}{\mathrm{d}t}\int_V \rho\, dV = \int_S \rho_s\,(\dot{a} - V_s)\, dS_s - \int_S \rho_\ell\,(\dot{a} - V_\ell)\, dS_\ell, \tag{20}$$

$$\frac{\mathrm{d}}{\mathrm{d}t}\int_V \rho H\, dV = \int_S \rho_s H_s\,(\dot{a} - V_s) + \mathbf{n}\cdot\mathbf{q_s}\, dS_s - \int_S \rho_\ell H_\ell\,(\dot{a} - V_\ell) + \mathbf{n}\cdot\mathbf{q}_\ell\, dS_\ell. \tag{21}$$

In the limit as $dx \to 0$ the amount of mass and energy stored within the control volume becomes negligible and we are left with the following relationships

$$\rho_s(a - V_s) = \rho_\ell(a - V_\ell), \tag{22}$$

$$\rho_s H_s\,(\dot{a} - V_s) + \mathbf{n}\cdot\mathbf{q_s} = \rho_\ell H_\ell\,(\dot{a} - V_\ell) + \mathbf{n}\cdot\mathbf{q}_\ell. \tag{23}$$

Since there is no motion in the solid, $V_s = 0$ and the mass conservation relation gives us a relationship for the fluid velocity. Substituting this relationship into the energy conservation equation and noting that $L = H_s - H_\ell$ we obtain the modified Stefan condition. These conditions are

$$V_\ell = \frac{\mathrm{d}a}{\mathrm{d}t}\left(\frac{\rho_\ell - \rho_s}{\rho_\ell}\right), \tag{24}$$

$$\rho_s L\frac{\mathrm{d}a}{\mathrm{d}t} = (\mathbf{q}_\ell - \mathbf{q_s})\cdot\mathbf{n}. \tag{25}$$

The addition of a fluid velocity on the liquid side adds an advective component to the governing temperature equation. The new model can be solved by a similarity solution

as a simple extension of the last section, but does not yield any new results. Since the temperature profile is homogeneous initially it must remain so for all time. On the other hand, if the liquid were under-cooled (as we shall see in the third lecture) or if we were melting the solid, the advective component would give a small correction to the interface speed as long as $\rho_s \approx \rho_\ell$.

References

[1] Taber, S. 1929. Frost heaving. *J. Geol.*, 37, 428-461.